Analysis of Functional Brain Network in MDD Based on Improved Empirical Mode Decomposition With Resting State EEG Data

Xuexiao Shao, *Graduate Student Member, IEEE*, Shuting Sun, *Graduate Student Member, IEEE*, Jianxiu Li, *Graduate Student Member, IEEE*, Wenwen Kong, Jing Zhu, *Member, IEEE*, Xiaowei Li, *Member, IEEE*, and Bin Hu, *Senior Member, IEEE*

***Abstract*— At present, most brain functional studies are based on traditional frequency bands to explore the abnormal functional connections and topological organization of patients with depression. However, they ignore the characteristic relationship of electroencephalogram (EEG) signals in the time domain. Therefore, this paper proposes a network decomposition model based on Improved Empirical Mode Decomposition (EMD), it is suitable for time-frequency analysis of brain functional network. On the one hand, it solves the problem of mode mixing on original EMD method, especially on high-density EEG data. On the other hand, by building brain function networks on different intrinsic mode function (IMF), we can perform time-frequency analysis of brain function connections. It provides a new insight for brain function connectivity analysis of major depressive disorder (MDD). Experimental results found that the IMFs waveform decomposed by Improved EMD was more stable and the difference between IMFs was obvious, it indicated that the mode mixing can be effectively solved. Besides, the analysis of the brain network, we found that the changes in MDD functional connectivity on different IMFs, it may be related to the pathological changes for MDD. More statistical results on three network metrics proved that there were significant differences between MDD and normal controls (NC) group. In addition, the aberrant brain network structure of MDDs was also confirmed in the hubs characteristic. These findings may provide potential biomarkers for the clinical diagnosis of MDD patients.**

***Index Terms*— Functional connectivity, major depressive disorder, high-density, improved empirical mode decomposition, resting state EEG.**

Manuscript received January 3, 2021; revised April 28, 2021; accepted May 19, 2021. Date of publication June 24, 2021; date of current version August 6, 2021. This work was supported in part by the National Natural Science Foundation of China under Grant 61632014, Grant 61802159, Grant 61627808, and Grant 61210010; in part by the National Basic Research Program of China through the 973 Program under Grant 2014CB744600; and in part by the Program of Beijing Municipal Science and Technology Commission under Grant Z171100000117005. *(Corresponding authors: Bin Hu; Xiaowei Li.)*

This work involved human subjects or animals in its research. Approval of all ethical and experimental procedures and protocols was granted by the Local Research Ethics Committee, Psychiatric Department, Lanzhou University Second Hospital, Gansu, China.

Xuexiao Shao, Shuting Sun, Jianxiu Li, Wenwen Kong, and Jing Zhu are with the Gansu Provincial Key Laboratory of Wearable Computing, School of Information Science and Engineering, Lanzhou University, Lanzhou 730000, China (e-mail: shaoxx19@lzu.edu.cn; sunsht17@lzu.edu.cn; lijx18@lzu.edu.cn; kongww20@lzu.edu.cn; zhujing@lzu.edu.cn).

Xiaowei Li is with the Gansu Provincial Key Laboratory of Wearable Computing, School of Information Science and Engineering, Lanzhou University, Lanzhou 730000, China, and also with Shandong Academy of Intelligent Computing Technology, Shandong 250000, China (e-mail: lixwei@lzu.edu.cn).

Bin Hu is with the Gansu Provincial Key Laboratory of Wearable Computing, School of Information Science and Engineering, Lanzhou University, Lanzhou 730000, China, and also with the CAS Center for Excellence in Brain Science and Institutes for Biological Sciences, Shanghai Institutes for Biological Sciences, Chinese Academy of Sciences, Shanghai 200031, China (e-mail: bh@lzu.edu.cn).

Digital Object Identifier 10.1109/TNSRE.2021.3092140

I. Introduction

DEPRESSION is a common illness worldwide with more than 264 million people affected, and is a leading cause of global disability and disease burden [1]. Major depressive disorder (MDD) is characterized by impairments of mood and cognitive function and is currently the second leading cause of death. Although some patients affected by major depression may recover within six months, up to 27% of patients do not recover and continue to develop chronic and refractory depression [2]. Therefore, understanding the underlying neurophysiology of MDDs is urgent in order to effectively diagnose and treat the disease [3].

With the development of imaging technology, many imaging technologies including electroencephalography (EEG), magnetoencephalography (MEG), functional magnetic resonance imaging (fMRI), and positron emission tomography (PET) etc. have been widely used to explore the mechanism of abnormal brain activity in depression and other mental illnesses. EEG is a technology that can record the electrical activity of the cerebral cortex, it can measure the electrical signals produced by many vertebral cells in the cerebral cortex, so as to objectively reflect the changes in the nerves in the brain. Compared with fMRI and PET, EEG has the characteristics of higher time resolution and low cost, which are favored by a large number of researchers. In recent years, analysis of functional brain connections based on EEG have been widely used in MDD, which explore regular activity patterns between

regions [4]. Kalpana *et al.* used 16-channel EEG data to study the abnormal functional brain network of EEG in MDDs resting state. Research based on graph theory found smaller weighted clustering coefficient (CC) and weighted characteristic path length (CPL) in the Alpha band [5]. In summary, most of the researches on brain function network based on EEG analyzed the changes of functional connectivity on different frequency bands [6], [7]. However, these studies ignored the characteristic relationship of EEG signals in the time domain. Therefore, it is meaningful to understand the changes in brain functional connectivity under different time domain.

Empirical mode decomposition (EMD) is a method that identify the vibration modes contained in the signal by the characteristic time scale [8]. Theoretically, it can be applied to the decomposition of any type of signal, so it has obvious advantages in processing non-stationary and non-linear data. Compared to other time-frequency methods (such as, wavelet decomposition and singular value decomposition), the advantages of EMD are as follows: 1) Adaptability. Compared with the wavelet transform that requires pre-selecting the wavelet basis function, the basis function of EMD can be automatically generated, so it is more suitable for analyzing complex EEG signals. 2) Maturity. The original signal can be obtained by adding all the decomposed components. It makes the process of signal decomposition reversible. This makes the performance of the EMD algorithm better than other traditional methods [9], [10]. In previous studies, the EMD method was applied to the time-frequency feature analysis of EEG signals, and the experimental results were excellent. Hassan and Bhuiyan [11] applied EMD method to extract the feature of EEG data, and used machine learning methods for classification, it is superior as compared to the state-of-the-art methods in terms of accuracy. Shen and Hu [12] used a feature extraction method based on EMD on four EEG databases, and the average classification results reached 83.27%, 85.19%, 81.98% and 88.07%. However, few studies have used time-frequency analysis methods in brain functional connectivity analysis (FCA). In our study, EMD was applied to the analysis of EEG to investigate the changes of abnormal brain functional connectivity in MDDs. It is worth mentioning that EMD is susceptible to the problem of mode mixing. Its local properties may produce oscillations of different scales in a single mode. Especially, when decomposing high-density EEG data, the problem of mode mixing becomes more serious. In order to solve this problem, this paper proposes a network decomposition model based on Improved EMD, which stabilizes the number of IMF obtained by decomposition and reduces information loss.

This study proposes a different method with the traditional FCA method, which uses an Improved EMD algorithm for high-density resting state EEG. The method realizes the mapping of multi-channel EEG to different intrinsic mode function (IMF), and further exploits IMF to study differences in brain network connectivity. Through the calculation of multiple coupling methods (e.g. correlation (CORR), coherence (COH), and phase lag index (PLI)) for different IMF sets, the functional connectivity matrixes are constructed [13]–[15]. Density method is used to construct the binary brain network. Then, network metrics (e.g. CPL, CC and Small World (SW)) computed from binarization network are used to study the changes of functional brain network in depression. Moreover, aberrant brain network structure in hubs characteristic is discussed in this study. And this study verified the effectiveness of these network metrics in distinguishing depression through machine learning methods, the experimental results showed that the classification accuracy of SW was 73.33% on IMF2. The result was equal or better than those on some traditional frequency bands. This paper proposes a time-frequency analysis of brain functional connectivity using the IMF instead of the traditional frequency band. These may provide a new idea to brain FCA and offer potential biomarkers in depression.

The rest of this study is organized as follows: Firstly, EMD and the Improved EMD methods are introduced in Section II; Then, the process of brain functional networks construction based on Improved EMD is shown in Section III; Next, the experimental results are analyzed and compared in Section IV; Finally, this study is concluded.

II. Methods

A. EMD

The EMD aims to generate highly local time-frequency estimates of the signal by decomposing the data into the finite sum of the IMF. The specific steps of EMD decomposition are as follows:

(1) Set $S_1 = x(t)$. And $x(t)$ represents the original input signal;

(2) Determine local extreme values (maximum and minimum);

(3) Obtain the envelope of the local maximum ($\upsilon_{\max}$) and local minimum ($\upsilon_{\min}$) by using cubic spline interpolation;

(4) Calculate the local average curve L_m:

$$L_m = \frac{\upsilon_{\max} + \upsilon_{\min}}{2} \tag{1}$$

(5) Calculate S_2:

$$S_2 = S_1 - L_m \tag{2}$$

(6) Repeat steps (2)-(5) until the SD reaches the predetermined value ε.

$$SD(k) = \frac{\|S_{k+1} - S_k\|^2}{\|S_k\|^2} < \varepsilon \tag{3}$$

(7) Set $c_1 = S_k$, c_1 is the first IMF; The steps (1)-(7) are called sifting.

(8) The first residue: $r_1 = x(t) - c_1$;

(9) Set r as the new input, repeat steps (1)-(7); Get $c_2 \ldots c_n$;

Finally, the input signal $x(t)$ can be decomposed into IMFs, until the remaining components become monotonic functions, the original signal can be represented as:

$$x(t) = \sum_{j=1}^{n} c_j + r_n \tag{4}$$

Among them, r_n is the remaining component of the n-th iteration.

EMD is widely used in EEG and other physiological signal analysis [16], [17]. However, mode mixing is still a

huge problem for EMD. The local characteristics of EMD may produce oscillations of different scales in one mode, or oscillations of similar scales in different modes, which is called "mode mixing." Fortunately, the ensemble empirical mode decomposition (EEMD) that adds auxiliary noise is proposed [18]. It adds normally distributed white noise to the original signal, and the signal after adding white noise was performed EMD decomposition on it. The formula is as follows:

$$x^i(n) = x(n) + w^i(n) \tag{5}$$

where $w^i(n)$ with i = 1,2,…, I represents different realizations of white noise.

Although EEMD is helpful to solve the problem of mode mixing, the residual noise generated by EEMD causes new troubles in modal decomposition [19]. Moreover, EEMD is also computationally expensive. All of them make EEMD unsuitable for practical applications.

B. Improved EMD

In order to better solve the problem of mode mixing in EMD, researchers have proposed many new and improved methods on this basis [11], [20] [21]. These all provide a reference for our method. In this study, we improved and enhanced the decomposition ability of EMD by adding a constant signal-noise ratio (SNR) setting to achieve the controllability of adding white Gaussian noise (WGN). Meanwhile, we used the estimation of the local mean (M(.)) to replace the estimation of the modal, and used the operator Φ_i to calculate the mode. All of these effectively solved the mode mixing problem. The process of Improved EMD method is as follows:

Firstly, the two operators are defined. One is the operator $\Phi_i(.)$ that generates the i-th mode of EMD. The other is the operator $M(.) = \frac{\sum_{i=1}^{I}}{I}$ that calculates the local mean of the applied signal.

Step1: Decompose the original signal X by EMD.

$$\Phi_i(.) = X + \lambda_0 w^i \tag{6}$$

where w^i represents different realizations of WGN. λ_0 represents a constant SNR value.

Step2: Calculate the first residue r_1 by $M(.)$.

Step3: Calculate the first IMF.

$$\widetilde{IMF_1} = X - r_1 \tag{7}$$

Step4: Estimate the second residual component based on the local mean $M(.)$.

$$r_2 = \left\{M(r_1 + \lambda_0 \Phi_1(w^i))\right\} \tag{8}$$

Step5: Calculate the second IMF.

$$\widetilde{IMF_2} = r_1 - r_2 \tag{9}$$

Step6: Calculate sequentially, and the k-th residual can be obtained.

$$r_k = \left\{M(r_{k-1} + \lambda_0 \Phi_k(w^i))\right\} \tag{10}$$

TABLE I
SYMBOL TABLE

Symbol	Explanation
$x(t)$	Original input signal
L_m	The local average curve
$v_{\max}$,$v_{\min}$	Local maximum and local minimum
r_n	The remaining component of the n-th iteration
$\Phi_i(.)$	i-th mode of EMD
$M(.)$	The local mean of the applied signal
w^i	Different realizations of WGN(i = 1,2,..,I)
λ_0	A constant SNR value
$\widetilde{IMF_k}$	k-th IMF
d_{ij}	The shortest path length of the node degree
a_{uv}	The number of edges connected to the node
t_i	The triangle number
C	Global CC of the test network
C_{rand}	Corresponding CC of the random network
L	Global CPL of the test network
L_{rand}	Corresponding CPL of the random network

Step7: The k-th IMF can be obtained.

$$\widetilde{IMF_k} = r_{k-1} - r_k \tag{11}$$

Step8: Repeat the above steps until the IMF becomes a monotonic function.

A new extreme value was calculated for the original signal with WGN in accordance with the normal distribution. And it realized signal fitting by calculating the local mean. In addition, the SNR is defined to control the amount of noise, so as to effectively reduce the amount of noise in the mode.

However, this method is mostly suitable for low-channel EEG data. For different EEG channels of the same person, or different people, the time-frequency domain of EEG signals is also different. Therefore, the problem of the number of different modes is inevitable. In order to solve these problems, we adopted the method of minimum threshold selection to drive the selection of IMFs based on high-density EEG data. The number of IMFs on each channel can be obtained by sequentially decomposing the EEG data of all channels. We chose the minimum threshold as the uniform number of IMFs output by each channel. And finally, the optimal number of modes can be determined in this study [22], [23].

III. CONSTRUCTION OF BRAIN FUNCTIONAL NETWORKS BASED ON IMPROVED EMD

A. Subjects

In this study, 30 subjects were used to analyze the results, including 15 MDD patients and 15 NC subjects. MDD patients recruited in this study were from the psychiatric department of the Lanzhou University Second Hospital, Gansu, China. The patient was diagnosed and recommended by at least one clinical psychiatrist. Participants in the NC group were recruited through posters. Established exclusion criteria included any type of neurological disorder, severe head injury and loss of consciousness, acute physical illness, and the presence of drug or alcohol abuse. To ensure the validity of the research, the exclusion criteria were strictly enforced before the experiment starts. This study was approved by

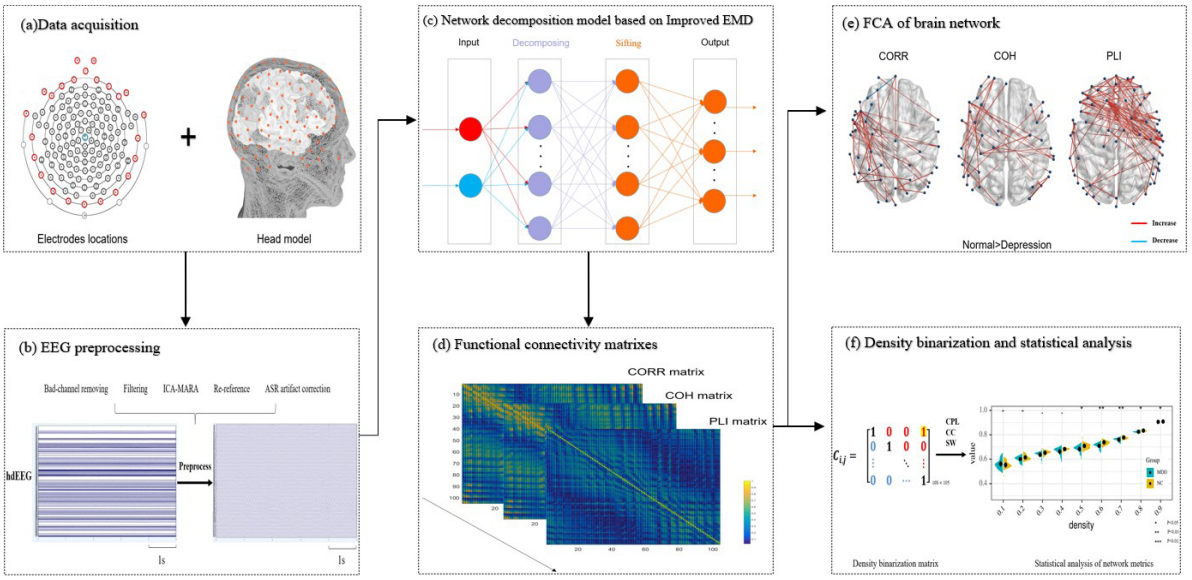

Fig. 1. The process of brain functional networks construction based on Improved EMD. (a) Data acquisition, it mainly introduces the position of the 105 channels electrode. (b) EEG preprocessing, the process of preprocessing are introduced. (c) Network decomposition model based on Improved EMD, the process of model is shown. (d) Functional connectivity matrixes, CORR, COH and PLI matrixes are calculated. (e) FCA of brain network, the functional connection analysis on different metrics is presented. (e) Density binarization and statistical analysis, it mainly introduces density binarization of the matrixes and statistical analysis of network metrics.

TABLE II
CHARACTERISTICS OF THE PARTICIPANTS IN THIS STUDY

Characteristic	MeanSD		p-value
	MDD	NC	
Number	15	15	–
Gender (Female/Male)	7F/8M	7F/8M	1.000
Age(years)	31.53±10.99	31.27±9.92	0.945
Education	13.80±4.16	15.40±3.56	0.267
Score of PHQ-9	18.20±3.76	2.67±2.27	**<0.001**

the local research ethics committee, and written informed consent from all subjects was obtained before the experiment started.

In this study, the relevant basic information statistics were made for the subjects. PHQ-9 was used to assess the degree of depression [24]. The chi-square was performed on the gender and T-test was used to evaluate the age, education level, and so on. The results were as follows in Tab.II.

The statistical results showed that there was no statistically significant difference in gender, age, education level between the two groups of subjects. There are statistical differences in the PHQ-9 scale for assessing depression, which meet the relevant experimental requirements. All the subjects used for the analysis of the results met all the conditions of this study, and they were rewarded after finishing the experiment. And all participants in the experiment should understand the related matters of the experiment and confirm the informed consent.

B. EEG Data and Preprocessing

The EEG acquisition equipment system in this experiment was provided by the American medical equipment manufacturer Electrical Geodesics, Inc (EGI). It contains a 128-channel EEG cap as shown in Fig. 1(a). The default reference electrode was the Cz electrode position, the sampling frequency was 250 Hz, the parameter of the online high-pass filter was 0.5 Hz, and the electrode impedance threshold was 50 kΩ. The EEG signals were continuously recorded for approximately 5 minutes.

The data preprocessing steps included EEG data channel selection, bad conduction detection, filtering, ocular artifact removal, ICA-based component removal, and artifact subspace reconstruction (ASR) artifact correction in time-domain. FIR bandpass filter was used to filter the EEG recording between 0.5-30hz [25], and REST was used to for re-reference [26]. The preprocessing was shown in Fig. 1(b). Through the above steps, the data preprocessing was completed. In this experiment, the 11-channel electrodes near the eyes were classified as ocular signals. In addition, due to signal noise of some electrodes, the 13-channel peripheral signals electrodes were removed manually. The final retained signal was 105 channels $(129 - (11 + 13) = 105)$. Details can be found in the supplementary materials.

In this study, due to the complexity of high-density data, we finally intercepted 12s sample data (105*250*12) from the stationary data 30s after each record for experimentation. The experimental tool was MATLAB R2016a.

C. Network Decomposition Model Based on Improved EMD

This paper decomposed a high-density resting state EEG data based on the Improved EMD method. In order to solve the problem of mode mixing, a hierarchical computing idea was used to simulate the mechanism of hierarchical information processing in the human brain. In essence, we regarded EEG

TABLE III
THE MATHEMATICAL FORMULATION OF THREE COUPLING METHODS IN THIS STUDY

Coupling methods	Mathematical formulation	Explanation
CORR	$\mathrm{CORR}_{xy}(\tau) = \frac{1}{N-\tau}\sum_{N-\tau}^{t=1}(\frac{x(t+\tau)-\bar{x}}{\sigma_x})(\frac{y(t)-\bar{y})}{\sigma_y})$	N is the total number of sampling points of the signal; τ is the time delay between two signals; $\bar{x}$ and σ_x represent the mean and standard deviation.
COH	$\mathrm{COH}_{xy} = \frac{\lvert\langle S_{xy(f)}\rangle\rvert}{\sqrt{\langle S_{xx(f)}\rangle \cdot \langle S_{yy(f)}\rangle}}$	$\langle . \rangle$ means the average value in the time interval; S_{xy} represents the cross power spectral density between signal x and signal y.
PLI	$\mathrm{PLI}_{xy} = \frac{1}{N}\left\lvert\sum_{N}^{t=1} sign(\Phi_x(t) - \Phi_y(t))\right\rvert$	Sign(t) represents the phase difference function.

signals as a combination of different signals. The bands of different IMF characteristics can be separated/classified based on EMD decomposition. Therefore, this paper proposed a network decomposition model which was suitable for high-density EEG data. It realized the normalization and division of EEG data of different channels into several fixed IMFs. Aiming at the problem of the number of different modes caused by multi-channel EEG data, we selected the minimum threshold screening method through statistical calculation of the number of decomposition components of each channel, so as to achieve the stability of the model output results. The process of network decomposition model was shown in Fig. 1(c). The details of our model are as follows:

(1) Input: we pack the MDD group and the NC group separately to form two 15*105*3000 input matrices, in which the amount of data for each person (105*3000), 105 is the electrodes number, 3000 is the data sampling points.

(2) Decomposing: we import two sets of data separately. For the data of each sample, we perform EMD decomposition in the order of channels. In this process, we add WGN with a constant SNR value in turn. In this way, we convert one person's data into multiple IMFs and form the class labels.

(3) Cyclic calculation: the step (2) is repeated, and the IMFs of different labels are classified into different IMF categories in order of sequence to form a new set.

(4) Sifting: Statistical calculations on the number of components decomposed by each channel of each sample are performed, the minimum threshold method is selected, and the set containing complete information is filtered out.

(5) Output: the output will contain the complete information of the owner. The output result is the final combination of 9 IMFs. And it is also the input signal for constructing the brain network.

After the processing of the above model, the high-density EEG data were decomposed into different IMFs on time-frequency domains, and the brain functional network was further constructed. Finally, the time-frequency domain analysis of these IMFs was realized.

D. Functional Networks Construction and Analysis

The brain functional networks are mainly composed of edges and nodes. First of all, we defined the electrode position of EEG as the nodes of the brain network. The number of nodes is 105. Moreover, the definition of the edge is based on the calculated connectivity between the electrodes. In this study, we selected three coupling methods CORR, COH and PLI to calculate functional connectivity matrixes as shown in Fig. 1(d). The formula was shown in Tab. III. The connectivity matrix was represented by an N x N square matrix, where the rows and columns represented the nodes in the connectivity network. The value in the connectivity matrix represents the strength of connectivity between nodes [27], [28]. The representation of the matrix is as follows:

$$C_{ij} = \begin{bmatrix} C_{11} & C_{12} & \cdots & C_{1n} \\ C_{21} & C_{22} & \cdots & C_{2n} \\ \vdots & \vdots & \ddots & \vdots \\ C_{n1} & C_{n2} & \cdots & C_{nn} \end{bmatrix} \tag{12}$$

In this study, the three functional connectivity matrixes were calculated for 9 IMFs to construct the brain network. And then, we averaged the functional connectivity matrixes between subjects to obtain the matrixes of each group and each IMF, so we can analyze the difference in the grouped functional connectivity matrixes as shown in Fig.1(e). Furthermore, the matrixes were converted into a binary matrix by selecting an appropriate threshold of density from 0.1 to 0.9(Increased by 0.1 each time). The relationship between the edges of the nodes was obtained as shown in Fig.1(f). Finally, we calculated the network metrics (CPL, CC and SW) for each binary brain network.

This study uses modular features and overall features to study the differences in brain network structure, such as: node degree, hubs, shortest path, triangle number and CPL, CC and SW network. Degree represents the number of edges directly connected to a node. The greater the degree of the node is, the more connections it has. And the position of the node is more important in the network. Its formula can be written as $k_i = \sum_{j=N} a_{ij}$, a_{ij} represents the number of edges connected to the node. The formula of the shortest path length of the node degree is as follows:

$$d_{ij} = \sum\nolimits_{a_{uv} \in g_{i \to j}} a_{uv} \tag{13}$$

Among them, $g_{i \to j}$ represents the shortest path between nodes, if there is no connection between i and j, then $d_{ij} = \infty$.

The characteristic path of the network measures the ability of the network to process information in parallel or the overall efficiency. The increase of the CPL shows that the efficiency of information transmission and interaction between brain regions is reduced. The calculation method is as follows:

$$CPL = \frac{1}{n}\sum\nolimits_{i \in N} L_i = \frac{1}{n}\sum\nolimits_{i \in N} \frac{\sum_{i \in N, j \neq i} d_{ij}}{n-1} \tag{14}$$

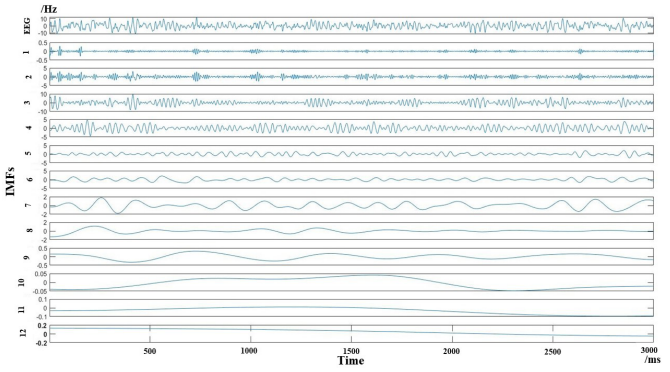

Fig. 2. The single-channel EEG signal is decomposed by Improved EMD.

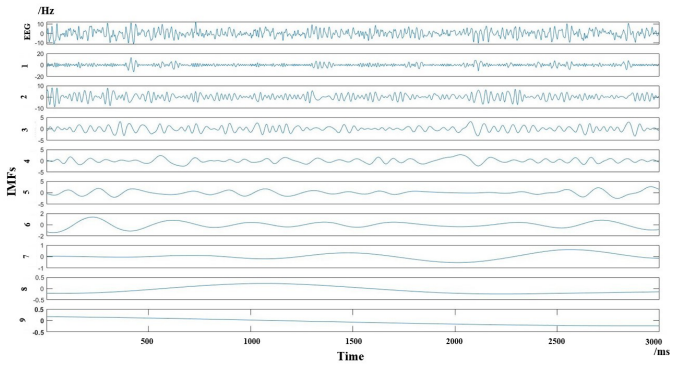

Fig. 3. The single-channel EEG signal is decomposed by original EMD.

The CC measures the degree of clustering of the network. The calculation method is as follows:

$$CC = \frac{1}{n}\sum\nolimits_{i\in N} C_i = \frac{1}{n}\sum\nolimits_{i\in N} \frac{2t_i}{k_i(k_i-1)} \tag{15}$$

Among them, t_i is the triangle number, which is the basis for calculating the degree of dispersion of the network.

The topological structure of the SW supports the differentiation and integration of brain information processing. The calculation method is as follows:

$$SW = \frac{C/C_{rand}}{L/Lrand} \tag{16}$$

Among them, C and C_{rand} represent the global CC of the test network and the corresponding random network respectively, and L and L_{rand} are the CPL respectively.

In this study, three network metrics (CPL, CC, and SW) were finally selected to study the difference between NC and MDD group, and the statistical tests were performed by T-test to analyze the degree of difference in the brain network structure. Especially, we adjusted the significance level of p values for multiple comparisons across networks metrics using a Bonferroni correction (family-wise error 0.05, n: the number of bands(IMFs or frequency bands), significance threshold $p < 0.05/n$) [29].

IV. Results and Analysis

A. The Problem of Mode Mixing

The problem of mode mixing is inevitable, when decomposing signal by EMD. Many researchers solved this problem by adding white noise. And, the methods were proved to be effective [9], [30]. In this study, we improved and enhanced the decomposition ability of EMD by adding a SNR setting to achieve the controllability of adding WGN. In order to show the effect of the experiment, we selected a single-channel EEG data from the sample data. We decomposed the single-channel EEG by using the original EMD and Improved EMD respectively. The single-channel EEG signal was decomposed by Improved EMD as shown in Fig. 2. And it was decomposed to 12 IMFs. It shows that each IMF waveform is relatively stable, and the difference between IMFs is obvious. However, the single-channel EEG signal was decomposed to 9 IMFs by

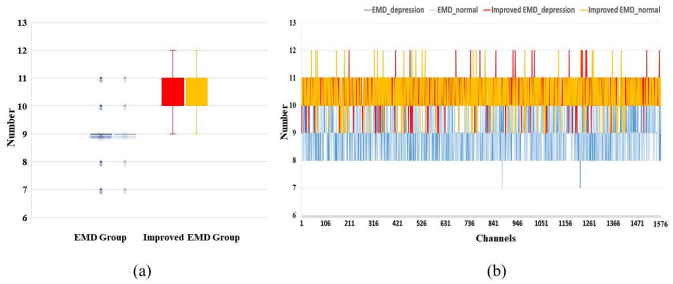

Fig. 4. Statistical analysis of the number on IMFs generated by the two methods in the model decomposition process. (a) The box plot of IMFs dispersion. (b) Distribution of the number of IMFs produced by all channels of EEG data.

original EMD as shown in Fig. 3. We can find the waveform is not fully decomposed by original EMD. And, the mode mixing is still existing between adjacent IMFs. In order to increase the interpretability of Improved EMD, we calculated the corresponding power spectrum by using the FFT algorithm for the data in Fig.2 and Fig.3 [31]. Details can be found in the supplementary materials. Experimental results showed that the power spectrum between adjacent IMFs on Improved EMD can be effectively distinguished, which is compared with the original EMD. Therefore, this also proves that the Improved EMD is effective to solve mode mixing problems.

In addition, this paper proposed a network decomposition model based on Improved EMD, it solved the problem of high complexity of high-density resting state EEG data. We used EMD and Improved EMD respectively in the model decomposition process. We tested the decomposition ability of model, through counting the number of IMFs generated in each channel. Distribution of the number of IMFs produced by all channels of EEG data was shown in Fig. 4(b). We can find that the Improved EMD can decompose more IMF compared to the original EMD. Moreover, the number of IMFs generated by EMD decomposition was excessively discrete as shown in Fig. 4(a). We can find that the number of IMFs decomposed by improved EMD is more concentrated and stable. On the one hand, it shows that the network decomposition model based on Improved EMD have stronger decomposition ability and robust. On the other hand, it also avoids the problem

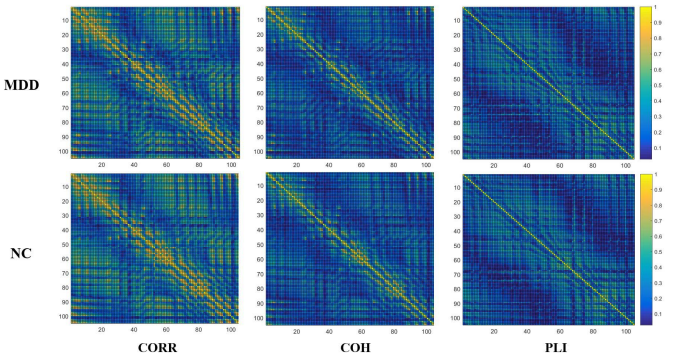

Fig. 5. Functional connection matrixes were calculated by three coupling methods on the full frequency band.

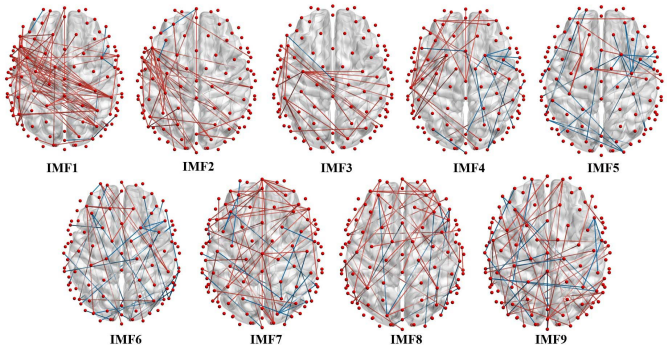

Fig. 6. The functional connection analysis of IMFs in CORR.

of excessive loss of information, when sifting under the minimum threshold. Therefore, these prove the advantages of our method.

B. Functional Connectivity Analysis

1) Functional Connectivity Matrixes: We calculated the CORR, COH and PLI connectivity matrix of the MDD and NC groups respectively on the full frequency band. The result was shown in Fig.5. Among them, the yellow area indicates a more active node (the larger value), which shows that it has a higher relevance or synchronization level, and the blue area indicates a lower degree of relevance between nodes. There is no obvious difference in the functional connection matrixes of the two groups. However, it can be found that the connectivity matrix constructed by CORR has a higher overall level of relevance or synchronization, and its yellow area is larger than the others from Fig.5. At the same time, the three matrixes (CORR, COH, PLI) all present some localized features. That is, there is a local aggregation effect between the high relevance area (yellow area) and the low relevance area (blue area) of nodes in different areas. For example: the high relevance area of nodes always appears near both sides of the main diagonal.

2) Distribution of Functional Connectivity: We also explored the differences in functional connectivity between groups under different coupling methods [32], [33]. We compared the values of the corresponding positions on the two sets of functional connection matrices one by one. The difference matrix between the two groups were filtered out by T-test ($P < 0.01$). The mean was used to represent their overall levels. Finally, we can get the difference of functional connectivity between the two groups ($M_{NC} - M_{MDD}$). It showed the difference in functional connection between the MDD group and the NC group in the three coupling methods on 9 IMFs.

The connectivity of the NC group was used as a standard to judge the connectivity changes of MDD. The red line indicates the decrease in connectivity, and the blue line indicates the increase in connectivity as shown in Fig.6. The functional connectivity of the MDD in whole brain was found to be declined in CORR, especially on IMF1, IMF2 and IMF3. However, it was found that the connectivity of the NC group was not

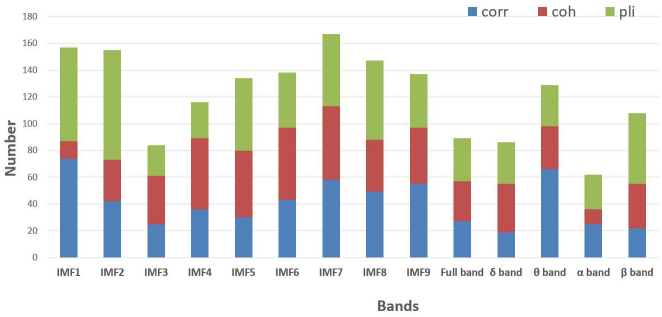

Fig. 7. The number of significantly different brain connections on different bands.

always higher than that of the MDD group. In particular, the study found that the functional connectivity of MDD was increased on IMF4-IMF9. Similar results were also confirmed on COH and PLI (See supplementary materials for details). This reflected the changes in MDD functional connectivity on different frequency bands [7]. And, it may be related to the pathological changes for MDD, which have the similar findings in literature [34]. Moreover, the functional connectivity analysis and location distribution results of IMF1 and IMF2 in PLI showed that the functional connectivity of the normal group was significantly higher than that of MDD, especially in the frontal and temporal regions. These all reflected the abnormal cognitive processing of MDD.

It is worth mentioning that we have done the same processing on the full frequency band and 4 individual frequency bands. The 4 individual frequency bands are Delta band (δ, 0.5 Hz-4 Hz), Theta band (θ, 4 Hz-8 Hz), Alpha band (α, 8 Hz-13 Hz) and Beta band (β, 13 Hz-30 Hz). In order to better compare the experimental effects of the two methods, we recorded the number of connections with significant differences in these bands. The result was shown in Fig.7. We found that the number of significantly different brain connections in IMFs was much larger than that in traditional frequency bands, especially IMF1, IMF2, IMF7 and IMF8. It showed that our method was superior to the traditional method in the analysis of functional connection. In addition, we also found that Theta band and Beta band also had better performance in the traditional frequency bands. These all provided a reference for us to identify the MDD.

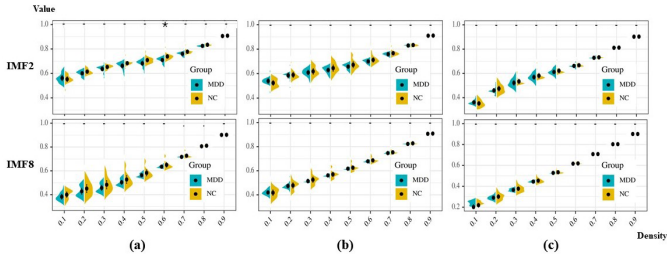

Fig. 8. The violin plots of CC on IMF2 and IMF8 in (a)CORR; (b)COH; (c)PLI. $*$ indicates family-wise error < 0.05 (Bonferroni corrected for multiple comparisons across network metrics, adjusted threshold $p < 0.006$).

C. The Difference on Network Metrics

1) Statistical Evaluate of Network Metrics: After analyzing the differences in the functional connectivity, we further calculated three network metrics based on the binarization matrixes. This research mainly analyzed the difference of network metrics from the two levels of network dispersion effect and aggregation effect. The network metrics include CPL, CC, SW. We used the T-test method to evaluate whether the MDD group and the NC group had statistically significant difference on network metrics, and adjusted the significance level of p values for multiple comparisons across network metrics using a Bonferroni correction (family-wise error 0.05, $n = 9$(IMFs); significance threshold $p < 0.05/9$, i.e. 0.006). The statistical results of CC were displayed on IMFs as shown in Fig.8. We only found that there were some significant differences in CC on IMF2. For CORR of IMF2 (density $= 0.6$), the degree in CC (0.74 ± 0.03) of NC was remarkably higher than that of MDD (0.71 ± 0.02, $p = 0.0041$).

In this study, we also carried out the differences analysis of density on CPL and SW, the results were shown significant differences of SW in IMFs. Among them, we found that CORR of IMF2(density $= 0.2$) had a significant difference between groups ($P = 0.0059$); In addition, there were significant difference between groups in COH of IMF8 (density $= 0.6$, $P = 0.0057$; density $= 0.7$, $P = 0.0019$). We can all find significant differences of network metrics on CC and SW in IMFs. This increases the possibility and credibility of using IMFs to explore network differences. Furthermore, we conducted the same experiment on the original EMD. We can only get 7 IMFs. Similarly, we perform statistical analysis on its network metrics (T-test, significance threshold $p < 0.05/7$, i.e. 0.007). We only found that significant differences of CPL on COH in IMF7(density $= 0.5$, $p = 0.0070$). Experimental results showed that the statistical results of IMFs on Improved EMD are significantly better than that on original EMD.

2) Correlation Between IMFs and Frequency Bands: In order to further verify our conclusions, we also conducted the same experiments on the traditional frequency bands(δ, θ, α and β bands). We only found some differences between groups on Beta band. For CORR of Beta (density $= 0.6$), the degree in CC (0.74 ± 0.02) of NC was remarkably higher than that of MDD (0.71 ± 0.02, $p = 0.0081$); For CORR of Beta(density $= 0.2$), the degree in SW(0.70 ± 0.28) of NC was remarkably higher than that of MDD (0.69 ± 0.26, $p = 0.0003$). It is consistent with the results of our method in IMF2. Compared with the traditional frequency division method, our method found significant differences in COH on IMF8. More refined difference results can be found on IMFs. This further proves that the EMD method is feasible. Of course, our method also has certain shortcomings, such as the inability to quantify the specific frequency domain range.

The frequency characteristics of EEG reflect a large amount of brain electrical activity information, but the local characteristics of the EEG signal cannot be obtained through frequency domain analysis. In fact, it cannot be extracted from the time domain or the frequency domain alone for some special features. Therefore, the time-frequency analysis method can better solve this problem. Temporal and spatial properties is provided by the IMF-based connectivity analysis compared to the study based on traditional frequency bands. These can be found from the decomposition process of Fig.2 and Fig.3. On the one hand, different IMFs can better represent the frequency domain characteristics of EEG signals without deviating from the specific time domain. On the other hand, different IMF have different time-scale characteristics, which makes each IMF include different time-frequency information. It is helpful to study the changes of the brain function network in different temporal and spatial properties. Moreover, the effective combination of EEG time domain and frequency domain information can improve the classification performance of EEG [35].

Besides, we conducted the same experiment on the full frequency band, and the results only found significant differences on CC of CORR(density $= 0.2$, $P = 0.0003$; density $= 0.3$, $P = 0.0041$; density $= 0.4$, $P = 0.0099$). From the perspective of the coupling method, the significant differences can always be found on CORR. Therefore, the performance of CORR was optimal compared to other coupling methods.

D. Analysis of Aberrant Brain Network Structure in Hubs Characteristic

According to some previous studies [6], we studied the distribution of hubs in the brain network in each brain area, and explored their differences between groups. Due to the analysis of the statistical results, we finally chose CORR to calculate the initial connectivity matrix, and the binarization method with a density of 0.2 to construct the brain network. The 105 electrode points were divided into 4 brain regions (No distinction between left and right). According to the best performance in the previous chapter, we further analyzed on the Theta band, Beta band, IMF2 and IMF8. The distribution of hubs in the MDD group and NC group was shown in Fig.9. The specific distribution of the electrodes on the brain regions can be found in the supplementary materials.

There were obvious differences in the activity of the hub nodes between the groups from Fig.9. The active hubs in NC group always had more than that in MDD group, which was consistent with the results of the previous studies [7], [36] [37]. This also further proved that MDD had aberrant cognitive processing [6]. The hub nodes distributed on the Beta band

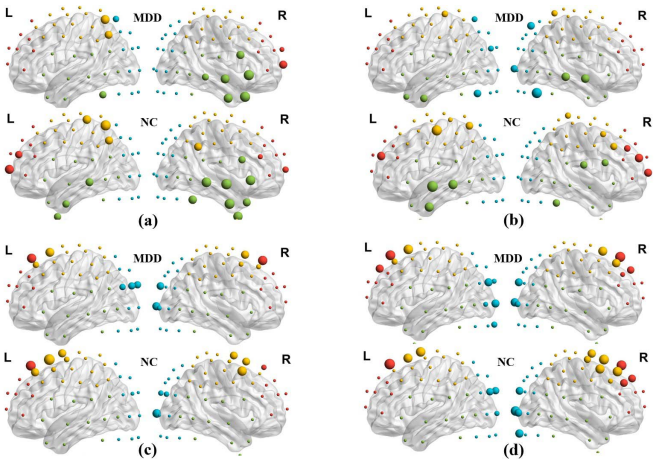

Fig. 9. The distribution of hubs nodes between MDD and NC group on (a) IMF2; (b) IMF8; (c) Beta band; (d) Theta band. Among them, the size of the node represents the degree of association of the corresponding brain regions. Red nodes represent frontal lobe, yellow nodes represent parietal lobe, green nodes represent temporal lobe, blue nodes represent occipital lobe.

and Theta band had no obvious difference between groups, and they were almost the same in left and right symmetry. However, we found that the activity of hubs in the central region of the NC group was significantly higher than that of the MDD group in the Beta band and Theta band. The central region of electrodes corresponds to the parietal lobe in the cerebral cortex, the parietal lobe is located at the posterior top of the cerebral hemisphere, and its main function is to regulate attention or allocate space for attention [38]. Therefore, this corresponds to the clinical manifestations of MDD, as inattention and memory loss. And we found that the NC group had a distribution of active hubs in the left frontal region and left temporal lobe region on IMF2, while the MDD group almost did not. In addition, the study found that obvious left-right asymmetry of MDD group on IMF2, which was similar to the literature [39]. It also supported the credibility of our method. Some current studies have revealed the differences in the left-right symmetry of the brain network between the two groups [40], [41], but the differences in brain regions related to emotion and cognitive functions should be better explained. The frontal lobe is located in the front part of the cerebral hemisphere and is mainly responsible for movement, emotion, and executive functions [42]. The function of the temporal lobe is to process auditory information and is also related to memory and emotion. Therefore, some changes in the frontal and temporal lobes may be an important cause of emotional instability in MDD. Especially, it was found on IMF8 that the NC group had the distribution of hubs in the frontal region, while the MDD group did not. This was contrary to the findings of the literature [43], it constructed a brain function network based on the COH of resting EEG data and showed that depressed people had higher connectivity in the prefrontal area, which can describe the enhanced role of hub nodes in the prefrontal area. This may be caused by different coupling methods, and the difference of experimental results will be relatively large. In addition, the activity of the hubs of the MDD group in the parieto-occipital region was higher than the NC group on the Beta band and IMF8. This may reflect that the occipital area of MDD is involved in emotional regulation and cognitive activities, but it needs to be further studied.

TABLE IV
CLASSIFICATION EVALUATION OF NETWORK METRICS IN THIS STUDY

Bands	Metrics	Accuracy	Precision	Recall	F-Measure	P value
IMF2	CC	60.00%	77.80%	60.00%	52.40%	0.1164
	SW	**73.33%**	75.10%	73.33%	72.90%	**0.0059**
IMF8	CC	**66.67%**	66.67%	66.67%	66.67%	0.2475
	SW	50.00%	50.00%	50.00%	49.50%	0.8772
β band	CC	53.33%	53.33%	53.33%	53.33%	0.0832
	SW	**80.00%**	82.30%	80.00%	79.60%	**$<$0.001**
θ band	CC	63.33%	77.80%	63.33%	59.70%	0.0772
	SW	**66.67%**	80.00%	66.70%	62.50%	0.0139

E. Classification Evaluation on Network Metrics

We further explored whether these network metrics can effectively distinguish depression through classification analysis. The network metrics was used as the features to distinguish the MDD group from the NC group. In this study, we calculated the network metrics (CC and SW) from the Beta band, Theta band, IMF2, IMF8 as the features for classification experiments. The Logistic model trees (LMT) algorithm was selected as the classifier, and Leave-One-Out (LOO) cross validation was used for classification. Accuracy, Precision, Recall, and F-Measure were used as a quantitative evaluation for classification performance of the above network metrics. The classification results were shown in the Tab.IV. The experimental tool was WEKA-3.8.4.

This research mainly used the CC and SW network metrics on CORR (density $= 0.2$) as the extracted features to perform classification experiments, and took the best result as the final classification result of the band. From Tab.IV, we found that the best classification effect was achieved on the Beta band, with a score of 80.00%. Moreover, we had also achieved good classification results on IMF2. The results were equal or better than the previous studies [12], [43], [44]. As for the difference in classification accuracy obtained on each spectrum, this may be related to the amount of information contained in each band. Besides, the performance of the features (SW) on the frequency bands was better than that on IMFs. Their significant difference (P value) on Beta band is better than that on IMF2. This may be the reason that cause the better classification result on Beta band. We can further study the different frequency bands or IMFs that contain information related to depression, as the objective indicators to distinguish depression patients from normal people. The classification results effectively supported the differences between the groups and the differences in hubs node activity discussed earlier, and provided reference value for studying brain network structure. At the same time, this also proved that it was possible to extract the network metrics as a method to distinguish MDD from NC by constructing a brain network. The result also showed that we used IMFs to alternate traditional spectrum analysis, which was also an effective method for analyzing and

constructing brain networks. The specific content may need further verification.

V. Conclusion

In order to solve the problem of high complexity of high-density resting state EEG data, this paper proposes a network decomposition model based on Improved EMD, it is suitable for time-frequency analysis of brain functional network. On the one hand, it solved the problem of mode mixing on original EMD method. On the other hand, it provided a new idea for the study of depression based on EEG. By building brain function networks on different IMFs, we can perform time-frequency analysis of brain function connections. Importantly, the time-frequency analysis method of high-density EEG data can be applied to future research. It can not only analyze the connectivity mode of the resting state network, but also detect the reconstruction mode of the dynamic functional network. At present, most EEG researches construct and analyze the functional connectivity of brain networks based on traditional spectrum analysis. However, it is also interesting to study the functional connectivity of brain networks in different time-frequency domains. Experimental results found more significant differences on network metrics compared to traditional frequency domain analysis. In addition, the aberrant brain network structure of MDD is also confirmed in the hubs characteristic. These all provide potential biomarkers for the clinical diagnosis of MDD.

Of course, this study also has some shortcomings, the EEG signal is a kind of neuronal oscillation, and the electrode points on the electrode cap as the node of the brain network will make the activation position of the brain region not accurate enough. In the future work, we should explore the distribution in the source space based on source location technology and fMRI, etc., so as to make the functional connectivity analysis of brain networks can be more refined and accurate.

References

[1] S. L. James *et al.*, "Global, regional, and national incidence, prevalence, and years lived with disability for 354 diseases and injuries for 195 countries and territories, 1990–2017: A systematic analysis for the global burden of disease study 2017," *Lancet*, vol. 392, no. 10159, pp. 1789–1858, 2018.

[2] A. J. Ferrari *et al.*, "Burden of depressive disorders by country, sex, age, and year: Findings from the global burden of disease study 2010," *PLoS Med.*, vol. 10, no. 11, Nov. 2013, Art. no. e1001547.

[3] A. Cipriani *et al.*, "Comparative efficacy and acceptability of 21 antidepressant drugs for the acute treatment of adults with major depressive disorder: A systematic review and network meta-analysis," *Lancet*, vol. 391, no. 10128, pp. 1357–1366, Apr. 2018.

[4] X. Li *et al.*, "A resting-state brain functional network study in MDD based on minimum spanning tree analysis and the hierarchical clustering," *Complexity*, vol. 2017, pp. 1–11, Oct. 2017.

[5] R. Kalpana and I. Gnanambal, "The analysis of nonlinear invariants of multi-channel EEG signal using graph-theory connectivity approach in patient with depression," *Asian J. Inf. Technol.*, vol. 15, no. 20, pp. 4106–4112, 2016.

[6] S. Sun *et al.*, "Graph theory analysis of functional connectivity in major depression disorder with high-density resting state EEG data," *IEEE Trans. Neural Syst. Rehabil. Eng.*, vol. 27, no. 3, pp. 429–439, Mar. 2019.

[7] H. Peng *et al.*, "Multivariate pattern analysis of EEG-based functional connectivity: A study on the identification of depression," *IEEE Access*, vol. 7, pp. 92630–92641, 2019.

[8] N. E. Huang, "The empirical mode decomposition and the Hilbert spectrum for nonlinear and non-stationary time series analysis," *Proc. Roy. Soc. London. A, Math., Phys. Eng. Sci.*, vol. 454, pp. 679–699, Mar. 1998.

[9] A. Arasteh, M. H. Moradi, and A. Janghorbani, "A novel method based on empirical mode decomposition for P300-based detection of deception," *IEEE Trans. Inf. Forensics Security*, vol. 11, no. 11, pp. 2584–2593, Nov. 2016.

[10] S. K. Hadjidimitriou and L. J. Hadjileontiadis, "EEG-based classification of music appraisal responses using time-frequency analysis and familiarity ratings," *IEEE Trans. Affect. Comput.*, vol. 4, no. 2, pp. 161–172, Apr. 2013.

[11] A. R. Hassan and M. I. H. Bhuiyan, "Computer-aided sleep staging using complete ensemble empirical mode decomposition with adaptive noise and bootstrap aggregating," *Biomed. Signal Process. Control*, vol. 24, pp. 1–10, Feb. 2016.

[12] J. Shen, X. Zhang, B. Hu, G. Wang, Z. Ding, and B. Hu, "An improved empirical mode decomposition of electroencephalogram signals for depression detection," *IEEE Trans. Affect. Comput.*, early access, Aug. 14, 2020, doi: 10.1109/TAFFC.2019.2934412.

[13] G. Nolte, O. Bai, L. Wheaton, Z. Mari, S. Vorbach, and M. Hallett, "Identifying true brain interaction from EEG data using the imaginary part of coherency," *Clin. Neurophysiol.*, vol. 115, no. 10, pp. 2292–2307, Oct. 2004.

[14] C. J. Stam, G. Nolte, and A. Daffertshofer, "Phase lag index: Assessment of functional connectivity from multi channel EEG and MEG with diminished bias from common sources," *Hum. Brain Mapping*, vol. 28, no. 11, pp. 1178–1193, 2007.

[15] L. Orgo, M. Bachmann, K. Kalev, M. Jarvelaid, J. Raik, and H. Hinrikus, "Resting EEG functional connectivity and graph theoretical measures for discrimination of depression," in *Proc. IEEE EMBS Int. Conf. Biomed. Health Informat. (BHI)*, Feb. 2017, pp. 389–392.

[16] H. Rao, S. Xu, X. Hu, J. Cheng, and B. Hu, "Augmented skeleton based contrastive action learning with momentum LSTM for unsupervised action recognition," *Inf. Sci.*, vol. 569, pp. 90–109, Aug. 2021.

[17] M. E. Torres, M. A. Colominas, G. Schlotthauer, and P. Flandrin, "A complete ensemble empirical mode decomposition with adaptive noise," in *Proc. IEEE Int. Conf. Acoust., Speech Signal Process. (ICASSP)*, May 2011, pp. 4144–4147.

[18] N. E. Huang, Z. Shen, and S. R. Long, "A new view of nonlinear water waves: The Hilbert spectrum," *Annual Rev. Fluid Mech.*, vol. 31, no. 1, pp. 417–457, 1999.

[19] F. Y. O. Abdalla, Y. Zhao, and L. Wu, "Denoising ECG signal by complete EEMD adaptive noise," in *Proc. IEEE Int. Symp. Signal Process. Inf. Technol. (ISSPIT)*, Dec. 2017, pp. 337–342.

[20] M. A. Colominas, G. Schlotthauer, and M. E. Torres, "Improved complete ensemble EMD: A suitable tool for biomedical signal processing," *Biomed. Signal Process. Control*, vol. 14, pp. 19–29, Nov. 2014.

[21] W. Jun, L. Yuyan, T. Lingyu, and G. Peng, "A new weighted CEEMDAN-based prediction model: An experimental investigation of decomposition and non-decomposition approaches," *Knowl.-Based Syst.*, vol. 160, pp. 188–199, Nov. 2018.

[22] N. U. Rehman, C. Park, N. E. Huang, and D. P. Mandic, "EMD via MEMD: Multivariate noise-aided computation of standard EMD," *Adv. Adapt. Data Anal.*, vol. 5, no. 2, Apr. 2013, Art. no. 1350007.

[23] X. Shao, B. Hu, Y. Li, and X. Zheng, "A study of sleep stages threshold based on multiscale fuzzy entropy," in *Proc. Int. Conf. Algorithms Architectures Parallel Process.*, 2018, pp. 239–248.

[24] K. Kroenke and R. L. Spitzer, "The PHQ-9: A new depression diagnostic and severity measure," *Psychiatric Ann.*, vol. 32, pp. 509–521, Sep. 2002.

[25] A. Widmann, E. Schröger, and B. Maess, "Digital filter design for electrophysiological data—A practical approach," *J. Neurosci. Methods*, vol. 250, pp. 34–46, Jul. 2015.

[26] D. Yao, "A method to standardize a reference of scalp EEG recordings to a point at infinity," *Physiol. Meas.*, vol. 22, no. 4, pp. 693–711, Nov. 2001.

[27] M. J. Paldino, Z. D. Chu, M. L. Chapieski, F. Golriz, and W. Zhang, "Repeatability of graph theoretical metrics derived from resting-state functional networks in paediatric epilepsy patients," *Brit. J. Radiol.*, vol. 90, no. 1074, Jun. 2017, Art. no. 20160656.

[28] W. Zheng *et al.*, "Multi-feature based network revealing the structural abnormalities in autism spectrum disorder," *IEEE Trans. Affect. Comput.*, early access, Jan. 1, 2019, doi: 10.1109/TAFFC.2018.2890597.

[29] A. Badhwar *et al.*, "Multivariate consistency of resting-state fMRI connectivity maps acquired on a single individual over 2.5 years, 13 sites and 3 vendors," *NeuroImage*, vol. 205, Jan. 2020, Art. no. 116210.
[30] A. Amann, R. Tratnig, and K. Unterkofler, "Detecting ventricular fibrillation by time-delay methods," *IEEE Trans. Biomed. Eng.*, vol. 54, no. 1, pp. 174–177, Jan. 2007.
[31] X. Zheng, X. Yin, X. Shao, Y. Li, and X. Yu, "Collaborative sleep electroencephalogram data analysis based on improved empirical mode decomposition and clustering algorithm," *Complexity*, vol. 2020, pp. 1–14, Jun. 2020.
[32] A. Griffa *et al.*, "Transient networks of spatio-temporal connectivity map communication pathways in brain functional systems," *NeuroImage*, vol. 155, pp. 490–502, Jul. 2017.
[33] H. Yu *et al.*, "Synchrony dynamics underlying effective connectivity reconstruction of neuronal circuits," *Phys. A, Stat. Mech. Appl.*, vol. 471, pp. 674–687, Apr. 2017.
[34] J. Wang *et al.*, "Local functional connectivity density is closely associated with the response of electroconvulsive therapy in major depressive disorder," *J. Affective Disorders*, vol. 225, pp. 658–664, Jan. 2017.
[35] B. Jie, M. Liu, and D. Shen, "Integration of temporal and spatial properties of dynamic connectivity networks for automatic diagnosis of brain disease," *Med. Image Anal.*, vol. 47, pp. 81–94, Jul. 2018.
[36] C. Sun *et al.*, "Mutual information-based brain network analysis in post-stroke patients with different levels of depression," *Frontiers Hum. Neurosci.*, vol. 12, p. 285, Jul. 2018.
[37] C.-A. Park *et al.*, "Decreased phase synchronization of the EEG in patients with major depressive disorder," in *World Congress on Medical Physics and Biomedical Engineering*. Berlin, Germany: Springer, 2007.
[38] Z. Bian, Q. Li, L. Wang, C. Lu, S. Yin, and X. Li, "Relative power and coherence of EEG series are related to amnestic mild cognitive impairment in diabetes," *Frontiers Aging Neurosci.*, vol. 6, p. 11, Feb. 2014.
[39] A. A. Fingelkurts, A. A. Fingelkurts, H. Rytsälä, K. Suominen, E. Isometsä, and S. Kähkönen, "Composition of brain oscillations in ongoing EEG during major depression disorder," *Neurosci. Res.*, vol. 56, pp. 44–133, Oct. 2006.
[40] T. Fan, X. Wu, L. Yao, and J. Dong, "Abnormal baseline brain activity in suicidal and non-suicidal patients with major depressive disorder," *Neurosci. Lett.*, vol. 534, pp. 35–40, Feb. 2013.
[41] G. C. Blackhart, J. A. Minnix, and J. P. Kline, "Can EEG asymmetry patterns predict future development of anxiety and depression?" *Biol. Psychol.*, vol. 72, no. 1, pp. 46–50, Apr. 2006.
[42] T. J. Whitford, C. J. Rennie, S. M. Grieve, C. R. Clark, E. Gordon, and L. M. Williams, "Brain maturation in adolescence: Concurrent changes in neuroanatomy and neurophysiology," *Hum. Brain Mapping*, vol. 28, no. 3, pp. 228–237, Mar. 2007.
[43] A. F. Leuchter, I. A. Cook, A. M. Hunter, C. Cai, and S. Horvath, "Resting-state quantitative electroencephalography reveals increased neurophysiologic connectivity in depression," *PLoS ONE*, vol. 7, no. 2, Feb. 2012, Art. no. e32508.
[44] H. Cai, Z. Qu, Z. Li, Y. Zhang, X. Hu, and B. Hu, "Feature-level fusion approaches based on multimodal EEG data for depression recognition," *Inf. Fusion*, vol. 59, pp. 127–138, Jul. 2020.